

Fluorescence dynamics of bovine serum albumin (BSA) conjugated CdZnS nanocrystallites

D. Mohanta^{1,2,a}, S.S. Narayanan³, S.K. Pal³, and A.K. Raychaudhuri³

¹ Nanoscience Laboratory, Department of Physics, Tezpur University, PO Napaam, Dist. Sonitpur, Assam-784 028, India

² Laboratory for Molecular Scale Engineering, 1415 Engineering Dr., Department of Electrical and Computer Engineering, University of Wisconsin-Madison, Madison, WI 53706, USA

³ S.N. Bose National Centre for Basic Sciences, Salt Lake, Kolkata 700 098, India

Received: 12 December 2007 / Received in final form: 1st March 2008 / Accepted: 7 April 2008
Published online: 30 May 2008 – © EDP Sciences

Abstract. We report on the production of composite semiconductor CdZnS nanoparticles by adopting an inverse micellar route, using bis (2-ethylhexyl) sulfosuccinate (aerosol-AOT) as surfactant and with a degree of hydration $w_0 = [\text{H}_2\text{O}] : [\text{AOT}] = 8.9$. Prior to bioconjugation (conjugation with bovine serum albumin (BSA)), the hydrophobic surface of the nanocrystals were made hydrophilic with thiol treatment (reacting with mercapto acetic acid). We compare photophysical nature of as prepared, thio-stabilized and bioconjugated CdZnS nanoparticles using absorption/emission spectroscopy and ultrafast photoluminescence decay measurements. The change-over from nonzero anisotropy (untreated) to zero anisotropy (bioconjugated) is assigned to the depolarized emission due to the surface reconstruction owing to BSA adsorption into the surface vacancies. Exploration of the dynamics of photophysical features would be promising for biomolecular sensing, labeling, and imaging applications.

PACS. 78.55.Et II-VI semiconductors – 78.67.-n Optical properties of low-dimensional, mesoscopic, and nanoscale materials and structures – 78.47.+p Time-resolved optical spectroscopies and other ultrafast optical measurements in condensed matter – 81.07.-b Nanoscale materials and structures: fabrication and characterization – 82.70.Uv Surfactants, micellar solutions, vesicles, lamellae, amphiphilic systems – 87.14.-g Biomolecules: types

1 Introduction

Over the years, intensive research has been fueled up to fabricate nanoscaled materials through bottom-up and top-down approaches. To protect nanoparticles from clustering and environmental degeneration, researchers have attempted synthesis in glass, polymers and zeolites, which have their own advantages and disadvantages [1–4]. On the other hand, reverse micellar (RM) route provides a unique way of obtaining narrow and uniform size distribution [5–7]. Inverse/reverse micelles are water-in-oil structures, considered as nanoreactors where molecules are allowed to react and grow to the desired dimension. Since, the size of the water pool is controlled by the degree of hydration (w_0) one can actually play with the size of the particles by just changing (w_0). Oil-in-water (micellar) cage like structures are very dynamic in nature, can exhibit Brownian motion and therefore, with time water soluble nanoparticles might grow in size while reaching equilibrium. On the other hand, inverse micellar structures

which contain isolated water pools can protect nanocrystals (NCs) more efficiently from clustering. Unfortunately, nanoparticles prepared in organic solvents though, exhibit better size control and protection against agglomeration, however, unsuitable for biomolecule attachment that requires NC surface to be hydrophilic. The easiest way to obtain a hydrophilic surface is by exchanging the hydrophobic surfactant molecules with bifunctional molecules that are hydrophilic on one end and bind to NCs with the other end. Treatment of thiols (-SH functional group) i.e., using mercaptoacetic acid/mercapto propanoic acid helps solubilization which can facilitate protein attachment through the covalent bonds. When reacted, the mercapto group binds to an atom and the polar carboxyl acid group renders the NCs water soluble. The free carboxyl group is also available for covalent coupling to the respective biomolecules (aminoacids, peptides, proteins, etc.). Carboxyl groups are negatively charged at neutral pH. The nanocrystals capped with carboxyl groups therefore, repel each other electrostatically. Following similar steps a number of reports have been published with regard to NCs-protein conjugation [8,9]. Recently, attempts

^a e-mail: best@tezu.ernet.in

have been made for applications such as fluorescence labeling, immunoassays including Förster resonance energy transfer processes in bioconjugate systems [10–12].

The present work reports on bovine serum albumin (BSA) protein conjugation with ternary CdZnS NCs and highlight nature of photoluminescence (PL) decay dynamics for such systems. The NCs unconjugated, and BSA-conjugated were characterized by steady state and ultrafast photoluminescence spectroscopy. The time resolved photoluminescence (TR-PL) was studied for excitation wavelength $\lambda_{ex} = 375$ nm and emission wavelength $\lambda_{em} = 420$ nm. The PL-decay patterns are analyzed through biexponential fits, owing to competitive radiative and nonradiative carrier recombination processes. The improvement of TR-PL anisotropic spectra of BSA-NCs system over unconjugated counter part is also discussed.

2 Experimental

Our experiment on bioconjugated NCs sample involves three major steps. First, producing colloidal CdZnS NCs by RM approach. Second, making NCs water soluble (hydrophilic) on reacting with thioglycolic acid, and finally treating with denatured BSA for obtaining BSA-NCs conjugates. The first step of RM route was adopted following method described by Pileni et al. [13]. For making reverse micelles, we have used bis (2-ethylhexyl) sulfosuccinate (aerosol-AOT, Aldrich & Co.) as the desired surfactant. In our experiment, the water-to-surfactant ratio (hydration degree, $w_0 = [\text{H}_2\text{O}] : [\text{AOT}] = 8.9$) was kept constant so that one would obtain average size of reverse micelles $r \sim 2 w_0 = 1.8$ nm and thus, capable of accommodating NCs of a few atomic clusters (Fig. 1).

440 mg of AOT was dissolved in 16.2 ml of *n*-heptane, followed by addition of 54 μl de-oxygenated water under vigorous stirring (~ 200 rpm) upto ~ 4 hrs. A clear, homogeneous microemulsion was obtained and nearly half of the volume was used for synthesis. It was further subdivided into three parts: (7 μl , 1M) Cd^{2+} and (7 μl , 1M) Zn^{2+} are added independently to each of the 2-ml parts where as freshly prepared (26 μl , 1M) S^{2-} was transferred to the third part (4.1 ml). The as-received mixtures containing Cd^{2+} and containing Zn^{2+} were added at once under stirring environment. Next, the third part containing S^{2-} was injected drop-wise by means of a micro-syringe. The as-prepared mixture was stirred overnight for maximum sulfide gas uptake and perfect nucleation of the desired $\text{Cd}_{0.50}\text{Zn}_{0.50}\text{S}$ NCs.

For thiol-stabilization, 1 ml Methanol was added drop-wise to 1 ml of the sample upto precipitation. The wet precipitate was wobbled well. Similarly, 0.1 ml thioglycolic acid (mercaptoacetic acid, Loba Chemi) was reacted with 1 ml of dimethylformamide (DMF) in a separate container. The above two precursors were gently mixed, vortexed and sonicated for about 45-mins. until a transparent solution was received. The as-prepared samples (thiol-stabilized NCs) were stored for 1-2 days prior to bioconjugation.

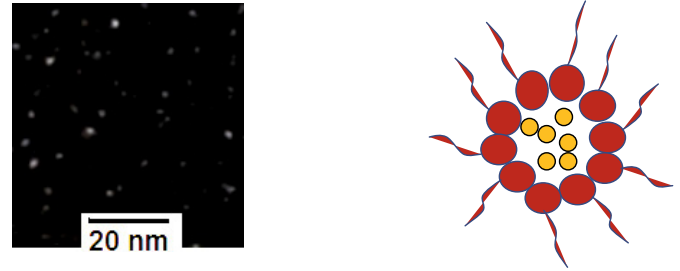


Fig. 1. (Color online) (a) Brightfield TEM and (b) schematic of CdZnS nanocrystallites (yellow spheres) grown in reverse micellar cage.

As a final step, chemically reduced BSA (Bovine Serum Albumin, Aldrich & Co.) was prepared by denaturing BSA in 1mM sodium borohydride in water at ~ 65 °C. Excess borohydride was removed by spontaneous decomposition by heating. Then, (2.6 ml, 197 μM) BSA was added to (0.4 ml, 25 μM) NCs for the bioconjugation purpose. After labeling, the test tubes were shaken well and made airtight with teflon. The NCs-BSA samples are allowed for incubation upto 3–5 days (65–70 °C). The incubated products were then extracted and placed in a centrifuge (~ 12000 rpm) for 5 hrs followed by decantation. The decant is our CdZnS NCs-BSA conjugate product, kept ready for subsequent experimentations.

At various steps of synthesis, samples were characterized and analyzed by various spectroscopic tools e.g. optical absorption and emission spectroscopy, time resolved photoluminescence spectroscopy, etc.

3 Results and discussion

The transmission electron micrograph (TEM) of CdZnS NCs along with schematic representation are shown in Figure 1. The TEM results depict nearly spherical, isolated nanoparticles with mean size calculated as 2.4 ± 0.5 nm. Optical absorption spectroscopy (OAS) provides information related to the onset of absorption, excitonic absorption, and size distribution. Figure 2 represents OAS of untreated, thiol-stabilized and BSA conjugated CdZnS-NCs. Using the formula due to Henglein et al. given by [14]:

$$2R = \frac{0.1}{0.1338 - 0.0002345 \lambda_e} \quad (1)$$

where λ_e corresponds to the onset of absorption edge, the average size of CdZnS nanoparticles was estimated as 2.9 nm (which corresponds to $\lambda_e = 425$ nm). This is possible in the sense that the size of the reverse micelles (dia $\sim 4 w_0$) which depends on the degree of hydration i.e. $w_0 = [\text{H}_2\text{O}]/[\text{AOT}] = 8.9$, should accommodate NCs of lower dimension (Fig. 1). Since the size of the NCs is within the strong confinement regime ($R < a_B$) electron and hole would confine independently. It is worth mentioning here that untreated CdZnS exhibits strong $1s-1s$ carrier absorption feature corresponding to ~ 383 nm and with an excitonic binding energy ~ 320 meV. However,

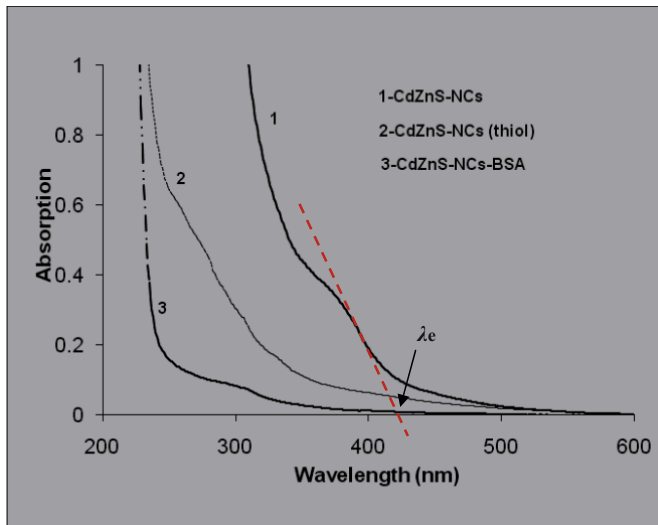


Fig. 2. (Color online) Optical absorption spectra of (1) untreated, (2) thiol-stabilized and (3) BSA conjugated $\text{Cd}_{0.5}\text{Zn}_{0.5}\text{S}$ -nanocrystals.

thiol treated and BSA conjugated CdZnS systems display featureless characteristics except tailing (Fig. 2). In other words, there is possibility of surface reconstruction in the NCs which prohibits exciton absorption. Typical FT-IR spectra (not shown) of untreated and thiol treated sample suggests that thiol treatment had led to the development of S-S bond at the expense of S-H bond, which is necessary for effective bioconjugation [8]. A scheme is shown in Figure 3.

The steady state photoluminescence (PL) spectra, shown in Figure 4 displays fluorescence response due to as-prepared, thiol-treated and BSA conjugated CdZnS NCs corresponding to $\lambda_{ex} = 375$ nm. The peak at ~ 420 nm is ascribed as band edge emission, being material dependent found to be independent of the excitation wavelengths (Fig. 5) and consistent to earlier reports [15]. The broad band ~ 470 – 550 nm is thought to be due to radiative charge recombinations at surface trap sites (each surface state corresponds to a definite energy level). Since, occurrence of carrier recombination at NCs' surface is greatly influenced by the arrangement of surface atoms/reconstruction owing to thiol treatment and bioconjugation, the trap-emission is quenched for such cases by ~ 7 fold (referring to crossing, inset Fig. 4b, c). The absence of trap related emission in bioconjugated CdZnS structures reveal adequate surface treatment which have led to the suppression of surface defects that might have arisen due to the presence of surface vacancies, adatoms, dangling bonds, etc. The chief reason for surface defects would have been chemical incompatibility of Cd (at. size ~ 148 pm) and Zn (at. size ~ 131 pm) atoms which can influence lattice parameter compared to pure CdS or ZnS.

Bioconjugated NCs are attractive for their ability to act as fluorescent probes [12]. Since fluorescence activation is a time dependent phenomena especially occurs in *ns-ps* time frame, it is important to investigate luminescence decay dynamics through time resolved photo-

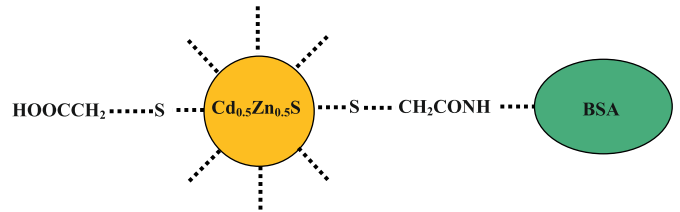


Fig. 3. (Color online) Schematic of CdZnS-BSA conjugation upon thiol-stabilization.

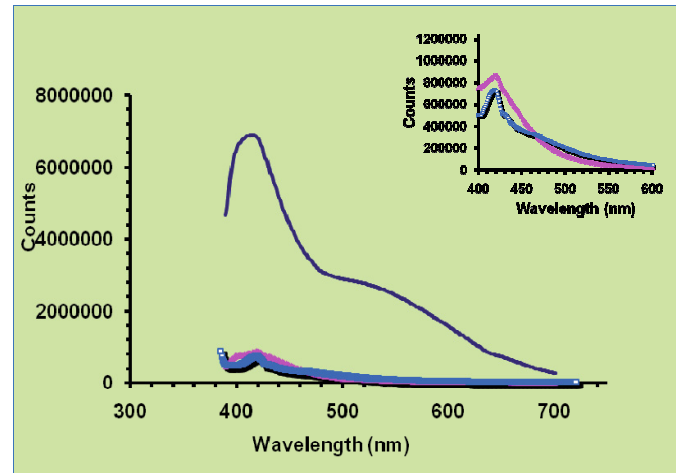


Fig. 4. (Color online) Steady state photoluminescence spectra (PL) of untreated (—), thiol-stabilized (\blacktriangle) and BSA conjugated (\square) CdZnS-NCs systems.

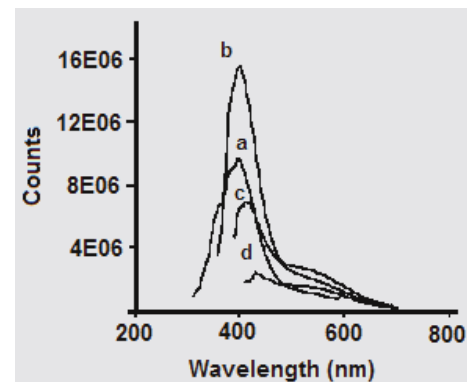


Fig. 5. PL emission response of CdZnS-NCs at various excitation wavelengths: (a) 299 nm, (b) 350 nm, (c) 375 nm, and (d) 400 nm.

bleaching study. Figure 6 is a time-resolved PL spectra of untreated and bioconjugate CdZnS nanoparticles. The bi-exponential fit to such systems must satisfy the relation:

$$y = y_1 e^{-t/\tau_1} + y_2 e^{-t/\tau_2}, \quad (2)$$

with τ_1 and τ_2 time constants of the rapid and slow processes and y_1 and y_2 being the intensities of corresponding processes, respectively. We believe that the rapid process deals with the direct $e-h$ recombination which

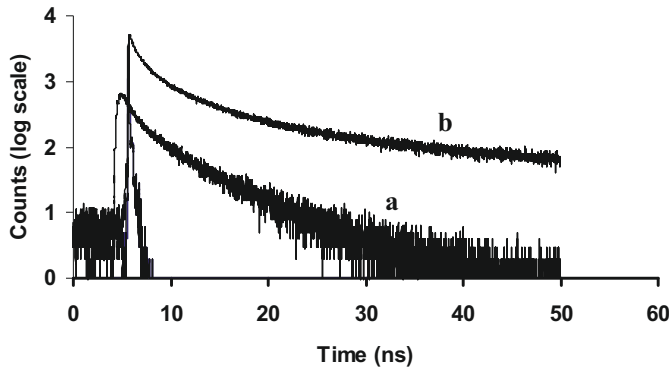


Fig. 6. TR-PL spectra of (a) untreated and (b) BSA conjugated CdZnS NCs.

occurs at the NC core through radiative paths. The slower process involves $e-h$ recombination via nonradiative channels (trap centers/surface states). For untreated CdZnS, $\tau_1 = \tau_2 = 21.2$ ns whereas BSA conjugates exhibit two distinct components $\tau_1 = 2.2$ ns and $\tau_2 = 20.1$ ns. It is clear that in unconjugated CdZnS system radiative and non-radiative processes are very much competitive and each contribute equally to the luminescence pattern. Since, unconjugate NCs have no surface protection, the emission is quenched faster than it is for BSA conjugate systems. Upon protein conjugation, surface reconstruction takes place by way of BSA binding to NCs surface which removes dangling bonds and surface defects from the NCs surface, thereby suppressing nonradiative channels. This is the reason CdZnS-BSA continues to emit longer period of time than untreated CdZnS. In other words, TR-PL spectra of CdZnS-BSA is truly biexponential where as untreated CdZnS actually displays single exponential characteristics.

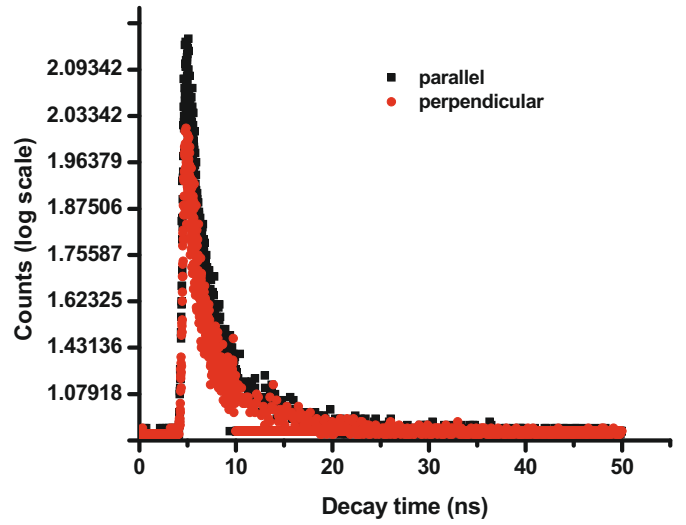
The time dependent decay of luminescence anisotropy provides additional information about the rotational motion and relaxation of the fluorescent material in a medium. In addition, the analysis of PL anisotropy decay is important to understand the nature of light emission from the NCs in view of their asymmetric shape and surface. The anisotropy decays as a sum of exponentials is expressed as [16,17]:

$$r(t) = (r_0 - r_\infty) \sum_i g_i \exp(-t/\phi_i) + r_\infty \quad (3)$$

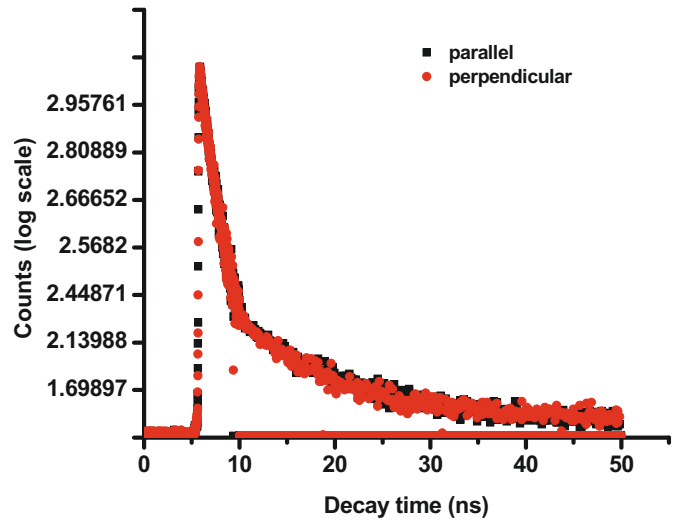
with r_0 and r_∞ represent the anisotropy value at $t' = 0$ and the limiting anisotropy, respectively. The functions g_i and ϕ_i are functions of the rates of rotation around the molecular axes of either untreated or bioconjugate systems. Upon plane polarized excitation, TR-PL anisotropic data was estimated from the components of the PL decay which are parallel and perpendicular to the excitation polarization given by [18,19]:

$$r(t) = \frac{I_{para} - I_{perp}}{I_{para} + 2 I_{perp}}. \quad (4)$$

The parallel and perpendicular polarization contributions (anisotropic spectra) are presented in Figure 7. In



(a)



(b)

Fig. 7. (Color online) (a) TR-PL anisotropic spectra of untreated CdZnS NCs. (b) TR-PL anisotropic spectra of BSA-CdZnS NCs.

untreated NCs, there is significant drop in the initial intensity for perpendicular polarization relative to parallel one (Fig. 7a). In contrary, perpendicular and parallel components display similar features for BSA-conjugated CdZnS nanoparticles (Fig. 7b). In other words, shape anisotropy or arrangement of surface atoms of the nanoparticles contributing to luminescence along mutually perpendicular directions are no longer realized in BSA linked nanoparticle system. In addition, conjugated CdZnS system displays truly biexponential features for both the polarizations, ensuing participation of distinct decay parameters (slow and fast components) responsible for photobleaching. Since there is a time delay between the excitation and detector response we have observed expected shift from $t = 0$ to $t \sim 5$ ns ($t' = 0$). There is significant anisotropy response around $t' = 0$

for both the samples. This could be due to initial response of the detector to parallel and perpendicular polarizations while cutting off the excitation wavelength. Also, it is advisable to accept $t' = 0$ at which PL signal reaches maximum. Using maximum values of intensity response e.g., $I_{para} = 136.97$ and $I_{perp} = 102.75$; we obtain anisotropy parameter as high as 9.99%. This nonzero anisotropy, noticed for untreated CdZnS nanostructures suggests the presence of some structural feature which directs the electronic transition along specific directions (polarized emission). Such nonzero anisotropies were noticed previously for a CdS colloidal composite with a dendrimer [15,20]. Also, polarized emission was reported in CdSe, ZnO and other nanosystems [21–23]. It was explained that in CdSe system, the polarized light emission occurs due to the resonance between interior and surface localized states while the asymmetric nature of elongated nanostructures was assigned to be the reason for directed $e-h$ recombination led polarized emission in ZnO system. A constant positive anisotropy is more useful if the nanoparticles are to be used as hydrodynamic probes [24]. Actually, beyond $t' = 0$, the photoluminescence anisotropy (PLA) decays due to orientational relaxation. In a polymer solution this happens through orientational diffusion of the polymer chains [25]. In the film, the decay of $r(t)$ is due to the intrachain and interchain excitation transfer, or creation of interchain states. Conversely, in our case, we notice $r(t)$ is almost zero for BSA conjugated CdZnS NCs. In other words, BSA environment protects CdZnS and removes shape asymmetry owing to the dimensions of BSA (14 nm \times 4 nm \times 4 nm) large compared to the later. It was known that the weak, fast decaying component of the anisotropy is associated with dipole-dipole-coupling-induced loss of orientation during (intrachain) energy migration along the polymer backbone [26,27]. We expect similar situation for our untreated CdZnS nanostructures (Fig. 7a) fabricated in an analogous RM environment. However, BSA-CdZnS NCs displays significant tailing in the TR-PL spectra which represents attestation of slow photobleaching (Fig. 7b). In addition, near-zero anisotropy (not shown) for $t' > 0$ reflects depolarization and therefore, absolute PL response due to distinctly different components.

If one considers the anisotropy decay of untreated CdZnS nanoparticles it is found to be strongly multiexponential, with most of the decay by the shorter correlation time ~ 0.35 ns. The presence of short correlation times is well known for fluorophores bound to proteins or membranes [28]. In these cases, the short correlation time is usually due to segmental motions of the fluorophores within large macromolecules. In case of NCs, segmental motion is irrelevant particularly when they are not conjugated with macromolecules. However, the anisotropy decay of BSA-CdZnS sample, upon exponential fit exhibits correlation time ~ 42 ns. This further confirms that even anisotropic decay study of BSA-CdZnS NCs exhibit slow decay and can help NCs protecting from photobleaching. Hence, with time bioconjugate sample will have greater environmental stability compared to untreated ones.

4 Conclusion

Following standard reverse micellar route, ternary CdZnS NCs were grown in control environment. Upon thiol-stabilization, they were conjugated to bovine serum albumin (BSA). Protein conjugated samples display biexponential PL characteristics due to involvement of slow ($\tau_2 = 20.1$ ns) and fast components ($\tau_1 = 2.2$ ns), compared to single exponential PL of untreated CdZnS nanocrystal ($\tau = 21.2$ ns). Nonzero anisotropy of untreated CdZnS NCs invokes polarized emission which might be due to the existence of asymmetric shape of NCs. With progression of time, BSA-CdZnS conjugates display vanishingly small anisotropy and is responsible for the depolarized emission owing to surface reorganization/construction. The extent of depolarized emission can be tunable with albumin content. In view of future application prospectives, quantitative analysis in this regard would help further understanding of biomolecular sensing and labeling.

One of the author (DM) would like to thank colleagues for valuable discussions while undergoing TR-PL measurements and Indian Academy of Science for financial assistance in the teacher fellowship scheme 2006-07.

References

1. Y. Wang, A. Suna, J. Meltugh, E.F. Hilniski, P.A. Lucas, R.D. Johnson, *J. Chem. Phys.* **92**, 6927 (1990)
2. A. Tanaka, S. Onari, T. Arai, *Phys. Rev. B* **45**, 6587 (1992)
3. H. Hofmeistera, G.L. Tan, M. Dubiel, *J. Mater. Res.* **20**, 1551 (2005)
4. W. Chen, R. Sammynaiken, Y. Huang, *Appl. Phys. Lett.* **88**, 5193 (2000)
5. M.P. Pileni, *J. Phys. Chem.* **97**, 6961 (1993)
6. H. Yang, P.H. Holloway, G. Cunningham, K.S. Schanze, *J. Chem. Phys.* **121**, 10233 (2004)
7. S. Li, V.T. John, G.C. Irvin, S.H. Rachakonda, G.L. McPherson, C.J. O'Connor, *J. Appl. Phys.* **85**, 5965 (1999)
8. W.J. Parak, D. Gerion, T. Pellegrino, D. Zanchet, C. Micheel, S.C. Williams, R. Boudreau, M.A. Le Gros, C.A. Larabell, A.P. Alivisatos, *Nanotechnology* **14**, R15 (2003)
9. H. Matssoussi, J.M. Mauro, E.R. Goldman, G.P. Anderson, V.C. Sundar, F.V. Milkulec, M.G. Bawendi, *J. Am. Chem. Soc.* **122**, 12142 (2000)
10. N.N. Mamedova, N.A. Kotov, A.L. Rogach, J. Studer, *Nano Lett.* **1**, 281 (2001)
11. C.-Y. Zhang, H.-C. Yeh, M.T. Kuroki, T.-H. Wang, *Nature Mater.* **4**, 826 (2005)
12. M. Bruchez, M. Moronne, P. Gin, S. Weiss, A.P. Alivisatos, *Science* **281**, 2013 (1998)
13. J. Cizeron, M.P. Pileni, *J. Phys. Chem.* **99**, 17410 (1995)
14. L. Spanhel, M. Hasse, H. Weller, A. Henglein, *J. Am. Chem. Soc.* **109**, 5649 (1987)
15. J.R. Lakowicz, I. Gryczynski, Z. Gryczynski, C.J. Murphy, *J. Phys. Chem. B* **103**, 7613 (1999)
16. G.G. Belford, R. Belford, G. Weber, *Proc. Natl. Acad. Sci. USA* **69**, 1392 (1972)
17. M.L. Martin-Fernandez, M.J. Tobin, D.T. Clarke, C.M. Gregory, G.R. Jones, *Rev. Sci. Instrum.* **69**, 540 (1998)

18. L.M. Herz, C. Silva, R.H. Friend, R.T. Phillips, S. Setayesh, S. Becker, D. Marisky, K. Müllen. *Phys. Rev. B* **64**, 95203 (2001)
19. A. Watanabe, T. Kodaira, O. Ito, *Chem. Phys. Lett.* **273**, 227 (1997)
20. K. Sooklal, L.H. Hanus, H.J. Ploehn, C.J. Murphy, *Adv. Mater.* **10**, 1083 (1998)
21. N.E. Hsu, W.K. Hung, Y.F. Chen, *J. Appl. Phys.* **96**, 4671 (2004)
22. M.G. Bawndi, P.J. Carroll, W.L. Wilson, L.E. Brus, *J. Chem. Phys.* **96**, 946 (1992)
23. F. Koch, D. Kovalev, B. Averboukh, G. Polisski, M. Benchorin, *J. Lumin.* **70**, 320 (1996)
24. J.R. Lakowicz, I. Gryczynski, Z. Gryczynski, K. Nwaczyk, C.J. Murphy, *Anal. Biochem.* **280**, 128 (2000)
25. S.A. van den Berg, G.W.'t Hooft, E.R. Eliel, *Chem. Phys. Lett.* **347**, 167 (2001)
26. A. Watanabe, T. Kodaira, O. Ito, *Chem. Phys. Lett.* **273**, 227 (1997)
27. T.-Q. Nguyen, V. Doan, B.J. Schwartz, *J. Chem. Phys.* **110**, 4068 (1999)
28. J.R. Lakowicz, *Principles of Fluorescence Spectroscopy*, 2nd edn. (Kluwer Academic/Plenum, New York, 1999)